Food Chemistry 372 (2022) 131221

Contents lists available at ScienceDirect

Food Chemistry

journal homepage: www.elsevier.com/locate/foodchem

Fabrication, characterization, and bioactivity assessment of chitosan nanoemulsion containing allspice essential oil to mitigate *Aspergillus flavus* contamination and aflatoxin B_1 production in maize

Anand Kumar Chaudhari, Vipin Kumar Singh, Somenath Das, Deepika, Nawal Kishore Dubey *

Laboratory of Herbal Pesticides, Department of Botany, Institute of Science, Banaras Hindu University, Varanasi 221005, India

ARTICLE INFO

Keywords:
Pimenta dioica essential oil
Nanoencapsulation
Antifungal
Antiaflatoxigenic
Safety profile
Food preservative

ABSTRACT

The direct incorporation of essential oils (EOs) into real food system faces numerous challenges due to high volatility, intense aroma, and instability. This research aimed to enhance the stability and bio-efficacy of *Pimenta dioica* essential oil (PDEO) through encapsulation in chitosan (CN) nanoemulsion. The nanoemulsion (CN-PDEO) was fabricated through ionic-gelation technique. CN-PDEO exhibited high nanoencapsulation efficiency (85.84%) and loading capacity (8.26%) with the particle size ranging between 18.53 and 70.56 nm. Bio-efficacy assessment results showed that CN-PDEO presented more effective antifungal and antiaflatoxigenic activity against *Aspergillus flavus* (AF-LHP-VS8) at lower doses (1.6 and 1.0 μL/mL) than the pure PDEO (2.5 and 1.5 μL/mL, respectively, $p < 0.05$). Additionally, CN-PDEO preserved model food (maize) from aflatoxin B_1 and lipid peroxidation without altering their sensory properties during storage with high safety profile ($p < 0.05$). Overall results concluded that CN-PDEO can be recommended for shelf-life extension of stored maize and other food commodities.

1. Introduction

The loss of postharvest agricultural food commodities by fungal and mycotoxin contamination has always been a serious problem throughout the world. *Aspergillus flavus* is by far the most prominent contaminant, and has been reported to cause huge loss of different agro-products, particularly during storage by producing a group of highly toxic metabolite called aflatoxins (Chaudhari et al., 2019). The consumption of aflatoxins poses severe risk in immune-compromised individuals because of their carcinogenic, teratogenic, mutagenic, and immunosuppressive effects, and hence, classified as group 1 carcinogen by the International Agency for Research on Cancer (Ostry, Malir, Toman, & Grosse, 2017).

Several chemical preservatives have been used to eliminate and degrade this ubiquitous contaminant; however, their excessive use many times may trigger the development of resistant races in fungal strains, residual toxicity to non-target organisms, and environmental pollution. For this reason, there has been a renewed scientific interest towards the use of natural preservatives. During the last decades, rather a wide range of plant derived essential oils (EOs) have been well documented and applied as food preservative to control large spectrum of mycotoxigenic fungi contaminating different stored food items (da Silva Bomfim et al., 2015; Chaudhari, Singh, Das, & Dubey, 2021).

Pimenta dioica (L.) Merr. (family: myrtaceae), popularly known as 'allspice' and valued for their fruits, is an important source of highly aromatic culinary spice. The fruits of allspice are commonly used as a source of EO, and contain α-Terpineol (30.31%) as a major compound (Chaudhari et al., 2020a). In our previous study, we had investigated the food preservative efficacy of *P. dioica* EO (PDEO) and found that PDEO have remarkable antifungal, antiaflatoxigenic, and antioxidant activities (Chaudhari et al., 2020a).

However, the direct application of PDEO in food system is relatively less preferred possibly due to water insolubility, strong aroma, high volatility, sensitivity towards oxidation, and negative impact on food organoleptic properties (Jemaa et al., 2017; Benjemaa et al., 2018). Nanoencapsulation of EO into efficient polymer matrix could mask the undesirable flavor, prevent volatility, increase aqueous solubility and stability, and minimize interaction with food matrices, thereby enhancing their bioavailability and bioactivity, while simultaneously enabling their controlled release (Chaudhari, Singh, Das, & Dubey, 2021). During last few years, chitosan (CN) has gained potential interest as encapsulating material due to non-toxicity, biodegradability,

* Corresponding author.
E-mail address: nkdubeybhu@gmail.com (N. Kishore Dubey).

https://doi.org/10.1016/j.foodchem.2021.131221
Received 15 June 2021; Received in revised form 1 September 2021; Accepted 23 September 2021
Available online 25 September 2021

biocompatibility, bioavailability, antimicrobial activity, and emulsion forming abilities (Ghaderi-Ghahfarokhi, Barzegar, Sahari, Gavlighi, & Gardini, 2017). Among various delivery systems, nanoemulsion synthesized through ionic-gelation (based on electrostatic interaction of CN with negatively charged phosphate groups of sodium-tripolyphosphate) is considered very promising carrier for water insoluble substances (particularly EOs) due to their ease of synthesis, sub-cellular particle size, improved bioavailability, kinetic stability, and sustained release property (Hasheminejad, Khodaiyan, & Safari, 2019).

So far there is no report available on the application of CN-nanoemulsion loaded with PDEO (CN-PDEO) with an aim to improve the quality of stored food items from fungal infestation, aflatoxin B_1 contamination, and lipid peroxidation. Hence, the current study was undertaken to i) develop a CN-nanoemulsion loaded with PDEO (CN-PDEO) through ionic-gelation technique using a cross-linker sodium-tripolyphosphate (S-TPP), ii) assess the antifungal and antiaflatoxigenic activity of CN-PDEO, iii) evaluate the *in vivo* preservative efficacy of CN-PDEO against aflatoxin B_1 production, and lipid peroxidation in a model food system (i.e. maize), and iv) finally mammalian safety profile assessment of CN-PDEO using oral acute toxicity test on male mice in order to introduce a novel antifungal source which could have potential for commercial exploitation in food industries.

2. Materials and methods

2.1. Materials and instruments

Chitosan powder (CN, deacetylation degree > 90%), sodium-tripolyphosphate (S-TPP), dichloromethane (DCM), acetic acid (glacial), acetonitrile, methylglyoxal (MG), thiobarbituric acid (TBA), trichloroacetic acid (TCA), perchloric acid, and Tween 80 were procured from Hi-Media Laboratories Pvt. Ltd., Mumbai, India. Nutrient media viz., Potato dextrose agar (PDA, the composition included 200 g **P**otato, 20 g **D**extrose, 15 g **A**gar powder and 1000 mL distilled water), and SMKY (the composition included 200 g **S**ucrose, 0.5 g **M**g$SO_4{\cdot}7H_2O$, 0.3 g **K**NO_3, 7 g **Y**east extract, and 1000 mL distilled water) were purchased from Sisco Research Laboratories Pvt. Ltd. (SRL), Mumbai, India.

The experimental investigation was based on instruments including homogenizer (T18263 Digital Ultra-Turrax, Germany), centrifuge (Remi CPR-4, India), ultrasonicator (Sonics Vibra Cell, USA), freeze-dryer (1–2 LD Plus, Australia), magnetic stirrer (IK-163, India), scanning electron microscope (Evo-18 researcher, Zeiss, Germany), sputter coater (Quorum, Q150R-ES, Lewes, UK), IR spectrometer (PerkinElmer, USA), UV–visible spectrophotometer (Hitachi-2900, Japan), trans-illuminator (Zenith, Agra, India), and atomic absorption spectrometer (AAnalyst 800, PerkinElmer, USA).

2.2. Fungal strains and maize samples

The most toxigenic strain of *Aspergillus flavus* namely AF-LHP-VS8 and 14 other storage fungi viz., *Aspergillus niger*, *Aspergillus luchuensis*, *Aspergillus sydowii*, *Aspergillus versicolor*, *Aspergillus fumigatus*, *Aspergillus repens*, *Penicillium chrysogenum*, *Penicillium italicum*, *Penicillium spinulosum*, *Fusarium oxysporum*, *Fusarium poae*, *Alternaria alternata*, *Cladosporium herbarum*, and mycelia sterilia were used in this study. These fungi were originally isolated from eight different varieties of maize samples in our previous study (Chaudhari et al., 2020a). Maize samples were collected from different locations of Uttar Pradesh and North-Eastern States of India and stored in sterile plastic bags for experimental purpose. The culture of AF-LHP-VS8 was maintained in the form of spore suspension in 0.1% solution of Tween 80, while of other fungi were maintained on PDA slants at 4 °C.

2.3. Chemical characterization of Pimenta dioica EO (PDEO)

The PDEO was characterized through GC–MS analysis according to our previous study (Chaudhari et al., 2020a). PDEO was introduced into gas chromatography (GC-2010, Shimadzu, Japan) having Rtx-5 column with dimensions 30 m × 0.25 mm × 0.25 μm. Oven temperature was raised from 40 °C to 330 °C (increase rate was set at 10 °C/min). Hydrogen gas was used as carrier gas (pressure 10 psi, split ratio 1:30, injector and detector (FID) temperatures 250 °C and 330 °C, respectively). GC–MS analysis was conducted through GC–MS (QP-2010 Plus, Shimadzu, Japan). The components were identified based on data presented in Wiley, NBS or with the published data (Adams, 2007).

2.4. Preparation of chitosan nanoemulsion loaded with PDEO (CN-PDEO)

CN-PDEO was fabricated through ionic-gelation technique of Hosseini, Zandi, Rezaei, & Farahmandghavi (2013) with some modifications. Firstly, CN solution was prepared by mixing 1.2 g pure CN (1%, w/v) in aqueous solution (120 mL) containing glacial acetic acid (1%, v/v) and stirred overnight at 25 °C. Tween 80 (HLB, 1.239 mL) was then added in the above solution and mixed for an additional 2 h at 45 °C. PDEO (0.06, 0.12, 0.18, 0.24 and 0.3 g) was suspended separately in DCM (4 mL) and this oil phase was gradually dropped into the CN solution (20 mL) during constant homogenization (13,000×*g*) for 10 min under ice-bath condition to achieve an oil in water (o/w) emulsion. For comparison, a control solution (CN-nanoemulsion) without PDEO was also prepared. Subsequently, 0.4% S-TPP was added drop-wise to the mixture and allowed to stir for 45 min. The formed nanoemulsions (CN-nanoemulsion and CN-PDEO) were collected by centrifugation (13,000×*g*) for 10 min, followed by subsequent washing with distilled water. Finally, nanoemulsions were sonicated with a sequence of 4 sec sonication and 4 sec rest for 8 min using ultrasonicator (20 kHz) and immediately freeze-dried at −62 °C for 3 days and kept at 4 °C until characterization.

2.5. Estimation of per cent nanoencapsulation efficiency and loading capacity

The nanoencapsulation efficiency and loading capacity of PDEO into CN-PDEO were determined by measuring the non-entrapped (surface) EO using UV–vis spectrophotometer following the protocol of Das et al. (2019) with slight modifications. The PDEO was extracted by dissolving 0.3 mL CN-PDEO in 2.7 mL ethyl acetate and centrifuged at 13000 × g for 10 min to obtain the supernatant solution. The absorbance of the sample was recorded spectrophotometrically at 309 nm (λmax of PDEO) and compared with the calibration curve (R^2 = 0.997). The per cent nanoencapsulation efficiency and loading capacity were calculated as follows:

$$\%\ \text{Nanoencapsulation efficiency} = \frac{\text{Total amont of PDEO loaded in CN} - \text{nanoemulsion}}{\text{Initial amount of PDEO}} \times 100$$

$$\% \text{ Loading capacity} = \frac{\text{Total amount of PDEO loaded in CN} - \text{nanoemulsion}}{\text{Weight of the lyophilized nanoemulsion}} \times 100$$

2.6. Characterization of nanoemulsion

2.6.1. Structure and size analysis

Scanning electron microscopy (SEM) analysis was carried out to examine the morphology and diameter of the prepared CN-nanoemulsion and CN-PDEO. The samples were diluted (10-folds) with Milli Q water; a small portion of it was placed on a cover-glass, and coated with gold film (Hosseini, Zandi, Rezaei, & Farahmandghavi, 2013). Subsequently, the morphology of the samples was examined in a Nova-nano SEM.

2.6.2. Functional groups and chemical structure analysis

Functional groups and chemical structures of CN, CN-nanoemulsion, PDEO, and CN-PDEO were characterized by Fourier Transform Infrared (FTIR) spectroscopic analysis using Perkin Elmer IR spectrometer. All samples except PDEO were mixed with KBr and squashed, and then recorded in the wave number ranging from 500 to 4000 cm^{-1} at a resolution of 4 cm^{-1} and 16 scans.

2.6.3. Crystallographic profile analysis

XRD patterns of CN, CN-nanoemulsion, and CN-PDEO were recorded in order to study their crystallographic profiles with a powder X-ray diffractometer. Patterns were obtained in the 2θ region from 5° to 50° with the step angle of 0.02° min^{-1} at a speed of 5° min^{-1}.

2.7. In vitro release properties of PDEO from CN-PDEO

In vitro release property of PDEO was determined in phosphate buffer saline (PBS) following the methodology of Hosseini, Zandi, Rezaei, & Farahmandghavi (2013) with little changes. Initially, CN-PDEO (1 mL) was put in a glass vial bearing 10 mL of PBS (pH 7). The mixture was then incubated at room temperature for 10 days. At specified time intervals, the sample was centrifuged and 1 mL of supernatant was withdrawn for analysis and replenished with the equal amount of fresh buffer to maintain the constancy. The absorbance of the sample was recorded at 309 nm. The release of PDEO was calculated by the following equation:

$$\text{Release}(\%) = \sum_{t=0}^{t} \text{Mt/Mo} \times 100$$

where,

Mt: amount of PDEO released at each sampling time, and

Mo: initial amount of PDEO encapsulated in the sample

2.8. Efficacy of PDEO and CN-PDEO against moulds and aflatoxin B_1 production

The antifungal activity of PDEO and CN-PDEO on AF-LHP-VS8 and 14 other storage moulds was evaluated using poisoned food technique with minor modifications (Chaudhari et al., 2020c). Different amounts of PDEO and CN-PDEO were pipetted aseptically into 9.5 mL PDA media in different Petri dishes to bring the final concentrations to 0.25–2.5 μL/mL and 0.2–1.6 μL/mL, respectively. 10 μL spore suspension of *A. flavus* at the concentration of 10^6 spores/mL and a 5 mm diameter disc from the periphery of the actively growing culture of remaining moulds was cut and inoculated into each Petri dish and then incubated for 7 days at 27 ± 2 °C. Control for un-encapsulated PDEO was prepared by addition of 0.5 mL Tween-20 (5%) into 9.5 mL PDA medium, whereas, control for CN-PDEO was prepared by adding CN-nanoemulsion to the PDA medium. It is important to note that antifungal activity against 14 other moulds was determined only at minimum inhibitory concentration (MIC) of PDEO (2.5 μL/mL) and CN-PDEO (1.6 μL/mL). The concentration of PDEO and CN-PDEO that completely inhibited the visible growth of treated fungi was considered as MIC. Following incubation, the fungal growth was determined by measuring colony diameter in Petri dish with reference to the treatment and control sets. The antifungal index was calculated according to the following equation:

$$\text{Antifungal index } (\%) = [(DC - DT)/DC] \times 100$$

where,

DC: average diameter of fungal colony in the control plate, and

DT: average diameter of fungal colony in the treated plate

To determine the inhibitory effect against aflatoxin B_1, required amounts of PDEO and CN-PDEO were aseptically pipetted into conical flasks bearing 24.5 mL of SMKY media in order to achieve final concentrations between 0.25 and 2.5 μL/mL and 0.2–1.6 μL/mL, respectively. Control for un-encapsulated PDEO was prepared by addition of 0.5 mL Tween-20 (5%) into 24.5 mL SMKY medium, whereas, control for CN-PDEO was developed by adding CN-nanoemulsion to the SMKY medium. For each concentration of PDEO and CN-PDEO, 25 μL spore suspension (10^6) of AF-LHP-VS8 was added and incubated for 10 days at 27 ± 2 °C. The media was extracted in chloroform and heated till complete dryness. The obtained residues were separately dissolved in 1 mL methanol and 50 μL of each sample was spotted onto the thin layer chromatography (TLC) plate and developed in the mobile phase comprising of toluene (90 mL), isoamylalcohol (32 mL), and methanol (2 mL). The aflatoxin B_1 content in the sample was determined using the methodology of Tian et al. (2012). The amount of aflatoxin B_1 was calculated according to the following equation:

$$\text{Aflatoxin } B_1 \text{ content } (\mu g/mL) = \frac{D \times M}{E \times L} \times 1000$$

where, D: absorbance of the sample

M: molecular mass of aflatoxin B_1 (i.e. 312 g/mol)

E: molar extinction coefficient (i.e. 21, 800 mol cm^{-1}), and

L: path length (1 cm used)

Further, the inhibition of aflatoxin B_1 was calculated from the following equation:

$$\% \text{ Inhibition} = [C_{AF} - T_{AF}/ C_{AF}] \times 100$$

where,

C_{AF}: mean aflatoxin B_1 content in the control, and

T_{AF}: mean aflatoxin B_1 content in the treatment

2.9. Antifungal mode of action of PDEO and CN-PDEO on A. flavus

2.9.1. Effect of PDEO and CN-PDEO on cellular ergosterol

Methodology of Tian et al. (2012) was followed to determine the ergosterol content in *A. flavus* cells. Briefly, known concentrations of PDEO (0.25–2.5 μL/mL) and CN-PDEO (0.2–1.6 μL/mL) were aseptically pipetted in different conical flasks containing 24.5 mL SMKY media and inoculated with 25 μL spore suspension of AF-LHP-VS8. After four days of incubation at 27 ± 2 °C, the grown fungal biomass was filtered, cleaned with distilled water and wet weight of the mycelium was determined. Thereafter, mycelia were transferred into test tubes and 5 mL 25% alcoholic KOH was added to it and vortexed for 2 min, followed by incubation on hot water bath for 2 h. Ergosterol was then extracted from the solution by adding a mixture of 2 mL distilled water and 5 mL *n*-heptane followed by vortex mixing for 2 min. After allowing the layers to separate for 30 min, the upper *n*-heptane was pipetted out and analyzed between 230 and 300 nm using UV–vis spectrophotometry. The amount of ergosterol was calculated as follows:

$$\% \text{ ERG} + \% \text{ 24(28) DHERG} = (\text{Abs}_{(282)}/290)/\text{pellet weight}$$

$$\% \text{ 24 (28) DHERG} = [\text{Abs}_{(230)}/518]/\text{pellet weight}$$

% ERG = (% ERG + % 24 (28) DHERG) – (% 24 (28) DHERG)

where,

290 and 518: E values (% cm^{-1}) determined for crystalline ergosterol (ERG) and 24(28) dehydroergosterol (DHERG), respectively.

The ergosterol inhibition was calculated from the following formula:

$$\% \text{ Inhibition} = \frac{\text{Ergostreol in control set} - \text{Ergosterol in treated set}}{\text{Ergosterol in control set}} \times 100$$

2.9.2. Effect of PDEO and CN-PDEO on mitochondrial membrane potential

The changes in mitochondrial membrane potential in PDEO and CN-PDEO treated AF-LHP-VS8 cells were monitored using the fluorescent dye rhodamine (RH123) (Tian et al., 2012). Briefly, RH123 was dissolved in PBS solution to prepare a 10 mg/mL stock solution. After being treated (overnight) with different concentrations (1/2MIC, MIC and 2MIC) of PDEO and CN-PDEO, the spore suspensions of AF-LHP-VS8 were harvested by centrifugation, washed, and re-suspended in PBS solution. RH123 with a final concentration of 2 μg/mL (prepared from the stock solution) was then added into the sample and incubated for 30 min under dark condition. The stained samples were further centrifuged, double washed, and re-suspended in the PBS solution and analyzed using fluorescence spectrophotometer at the excitation and emission wavelengths of 488 nm and 525 nm, respectively.

2.9.3. Effect of PDEO and CN-PDEO on cytoplasmic constituents release

The cellular constituent release was measured in terms of ion's leakage (Ca^{2+}, Mg^{2+} and K^{+}) and loss of 260 (nucleic acid) and 280 nm (proteins) absorbing materials according to the protocol of Das et al. (2019) with slight modifications. To evaluate the amount of cellular ions, 5-days old mycelia of test fungus were filtered, double washed and re-suspended in 0.85% saline solution. The suspensions were then treated with different concentrations (1/2MIC, MIC and 2MIC) of PDEO and CN-PDEO and incubated overnight at 27 ± 2 °C. Suspensions without PDEO and CN-PDEO were served as controls. After incubation, the contents were centrifuged (5,000 × g) and the resulting supernatants were analyzed for respective ions using atomic absorption spectrophotometer. The contents of nucleic acid and protein released were measured by reading absorbance of the above supernatants at 260 and 280 nm, respectively using a UV–visible spectrophotometer.

2.10. Antiaflatoxigenic mode of action of PDEO and CN-PDEO on *A. flavus*

The antiaflatoxigenic mode of action was investigated by measuring the level of intracellular methylglyoxal (MG, an important metabolite inducing aflatoxin B_1 biosynthesis in the *A. flavus* cells) following Upadhyay et al. (2018) with few modifications. In brief, 0.3 g cultured biomass of test fungus was inoculated in SMKY medium containing different concentrations of PDEO (0.25–2.5 μL/mL) and CN-PDEO (0.2–1.6 μL/mL). After overnight incubation at 27 ± 2 °C, the mycelia were crushed with 3 mL of 0.5 M perchloric acid, incubated on ice bath for 15 min, and centrifuged at 13,000×*g* for 10 min. The obtained supernatants were then neutralized by drop wise addition of saturated potassium carbonate and centrifuged again at the same rotation speed. The supernatants were used for the determination of MG at an absorbance of 341 nm.

2.11. *In vivo* aflatoxin B_1 inhibitory efficacy of PDEO and CN-PDEO in food system

In order to investigate the *in vivo* efficacy of PDEO and CN-PDEO as novel food preservative, its effect against *A. flavus* producing aflatoxin B_1 in stored maize samples was analyzed using Chaudhari et al. (2020b). For this, test maize grains were stored in closed plastic containers (500 mL) and grouped in three different sets. In one set (inoculated treatment at MIC), the sample was treated with MIC concentration of PDEO (2.5 μL/mL) and CN-PDEO (1.6 μL/mL) followed by inoculation with 500 μL spore suspension of AF-LHP VS8. In another set (inoculated treatment at 2MIC), the sample was treated with 5.0 μL/mL of PDEO and 3.2 μL/mL of CN-PDEO followed by inoculation with same amount of spore suspension. A control group (third set), containing spore suspension without PDEO and CN-PDEO was also used. All samples were incubated at 25 °C for one year and aflatoxin B_1 content in sample was analyzed by homogeneous liquid–liquid extraction coupled to high performance liquid chromatography (HPLC) following the protocol of Sheijooni-Fumani, Hassan, & Yousefi (2011). The analyses were carried out by using Waters 515 HPLC system with fluorescent detector having excitation and emission of 360 and 440 nm, respectively. The chromatographic separation was carried out on a reverse phase C18 column using different ratios of mobile phase (methanol: acetonitrile: Milli Q water, 17:19:64, v/v/v) and delivered under isocratic condition with the flow of 1.2 mL/min. The limit of detection (LOD) was 12.5–500 ng/50 mL. Pure aflatoxin B_1 dissolved in methanol (1 μg/mL) was used for the preparation of standard curve.

2.12. Determination of lipid peroxidation in stored maize

The extent of lipid peroxidation was measured in term of malondialdehyde (MDA) content following the method reported by Deepika, Chaudhari, Singh, Das, & Dubey (2021) with minor modification. For this, 5 g well milled maize sample (from the above-mentioned experiment) was added into 20 mL 0.37% TBA homogenized in 15% TCA and 0.2 N of the hydrochloric acid. The mixture was vortexed and heated on hot water bath for 30 min to develop color, cooled rapidly in cold water, and centrifuged at 5,000×*g* for 5 min. The absorbance of the supernatant was recorded both at 600 and 532 nm using UV–vis spectrophotometer.

2.13 . Phytotoxicity assessment of PDEO and CN-PDEO in maize

The phytotoxicity assay was performed in terms of seed germination test (Kordali et al., 2008). For this, four viable seeds from stored maize samples treated with MIC dose of PDEO (2.5 μL/mL) and CN-PDEO (1.6 μL/mL) were taken and placed equidistantly in Petri plates containing moistened blotting papers. The plates were incubated in BOD chamber for one week and the lengths of the plumules were recorded.

2.14. Safety profile assessment: Oral acute toxicity study of PDEO and CN-PDEO

Six-week old Swiss albino male mice (average weight 30) were procured from the Department of Zoology, Banaras Hindu University, India. The animals were allocated in groups of 10 per cage under controlled laboratory condition. Serial doses (ranging from 100 to 1000 μL/30 g body weight) of PDEO and CN-PDEO were administered orally to each group of the mice. One group, serving as positive control, received Tween 80 and CN-nanoemulsion and one serving as negative control received distilled water. All groups were then placed under observation and symptoms of toxicity were recorded during 6–24 h (Das, Singh, Dwivedy, Chaudhari, & Dubey, 2021). By the end of the period, dead mice were counted to determine median lethal dose (LD_{50}) by the logarithmic regression analysis of the dose–response curve.

2.15. Sensory analysis of PDEO and CN-PDEO treated maize

The consumer acceptance of maize samples treated with MIC and 2MIC of PDEO and CN-PDEO was evaluated for sensory analysis by the panel of ten untrained individuals (5 men and 5 women between the age group of 25–40 years from Department of Botany, Banaras Hindu University, Varanasi, India) using 7-point hedonic scale (7: extremely like, 6: moderately like, 5: slightly like, 4: neither like nor dislike, 3: slightly dislike, 2: moderately dislike, and 1: extremely dislike) (Chaudhari

et al., 2020c). Five different attributes viz., color, texture, aroma, taste, and overall acceptability were evaluated for sensory analysis. Maize samples without any treatment were served as control. Samples were served to the panellists in a transparent glass plate and coded with two digit codes.

2.16. Statistical analysis

Results were expressed as mean values ± standard error. The statistical differences among groups were identified by one-way ANOVA followed by Tukey's B multiple comparison test ($P < 0.05$) using SPSS version 16.0 (Chicago, IL, USA).

3. Results and discussion

3.1. Chemical characterization of PDEO

The diversity of volatile compounds of EOs is the most significant parameter affecting biological properties of the oils. The result obtained from the GC–MS analysis of PDEO in our previous study revealed the presence of α-terpineol (30.31%), β-linalool (6.75%), γ-terpinene (4.64%), and eucalyptol (3.42%) as the major components (Chaudhari et al., 2020a). However, Dima, Cotârlet, Alexe, & Dima (2014) reported that main components of EO obtained from *Pimenta dioica* were eugenol (68.06%), methyl eugenol (9.37%), β-caryophyllene (8.73%), and α-phellandrene (6.67%). This variation in the result could be related to the different collection time, age of the plant, geographical conditions, and different extraction process. In the present investigation, dried fruits of *P. dioica*, collected in summer season have been used for the extraction of EO. However, in some parts of the Asiatic and European countries, fruits of *P. dioica* get matured in the months of September to October, which are used for extraction of EO. Hence, seasonal variation along with the geographical alteration has been pointed out as major factor for variation in chemical composition of EO. Moreover, long dry season, slow oxygen uptake during fruit maturation (leading to modification of plant biosynthetic metabolism), and variation in microclimatic conditions viz., temperature, precipitation, and atmospheric pressure have also been linked with the alteration in chemical compositions of EO (Pitarević, Kuftinec, Blažević, & Kuštrak, 1984; Barata et al., 2011). On the other hand, the difference in composition might also be influenced by process of nanoencapsulation. For instance, Hussein et al. (2017) during encapsulating the rosemary EO into chitosan and alginate reported reduction in the composition of α-pinene and camphene, while enhancement in the composition of others (1,8-cineol and α-terpineol). The authors also suggested that these changes in the chemical composition might be linked to the conjugation of EO with the encapsulating polymers. The substantial impact of encapsulation on the chemical composition of EO was also demonstrated by Ali, Al-Khalifa, Aouf, Boukhebti, & Farouk (2020), where they found that the hydrodistillated EO of *Origanum glandulosum* showed the presence of carvacrol (26.29%), γ-terpinene (23.43%), thymol (19.52%), p-cymene (11.67%), and α-terpinene (3.02%) as the major components and were found in very least concentrations or not identified at all after nanoencapsulation. However, some compounds like borneol (0.10%) and α-terpineol (0.49%) which has been found in very least concentration were present in high amounts after nanoencapsulation. Such differences in the EO compositions might be attributed to the intensity of homogenization used during nanoemulsion preparation. Hence, further research should be conducted in order to establish the role of different conditions, which, in spite of conserving the overall stability of EO, could also maintain their standard composition in the nanoformulation.

3.2. Preparation of chitosan nanoemulsion loaded with PDEO (CN-PDEO)

CN-PDEO was prepared by ionic-gelation technique via mixing the homogenous solution of CN and the cross-linker S-TPP. Tween 80 was used as emulsifier, because EOs have strong interactions with non-ionic emulsifier that is quickly adsorbed at the o/w interface and offers outstanding stability to the emulsion (Hossain et al., 2019). CN was selected as a nanocarrier for the selected EO because of their non-toxicity, biodegradability, compatibility, and antimicrobial properties against different food borne contaminants (Das, Singh, Dwivedy, Chaudhari, & Dubey, 2021). In addition, safety and rapid emulsifying ability of S-TPP are the vital properties that make them a suitable cross-linking agent for CN. In aqueous medium, CN is soluble under acidic pH due to the protonation of amine groups and acts as cationic polyelectrolyte, which favours its strong electrostatic interaction with cross-linker S-TPP, leading to the formation of CN-nanoemulsion. CN-nanoemulsion is soluble in water and presents a structure that allows the entrapment of EO, thus making it to function as suitable nanocarrier.

3.3. Estimation of per cent nanoencapsulation efficiency and loading capacity

The per cent nanoencapsulation efficiency and loading capacity of PDEO into CN-PDEO are presented in Table 1. The encapsulation efficiency was increased from 45.81% to 85.84% when CN to PDEO ratio ranged from 1: 0.2–1: 1, respectively. Similarly, the loading capacity was increased from 0.68% to 8.26% with the increasing CN to PDEO ratio from 1: 0.2–1: 1, respectively, which means that the more CN in the solution, the greater would be the encapsulation efficiency and loading capacity. Our result is in accordance with the previous investigation of Singh, Das, Dwivedy, Rathore, & Dubey (2019) regarding encapsulation of *Ocimum sanctum* EO into chitosan nanobiopolymer suggesting increase in initial content of EO in loading capacity (2.01%-5.28%) and encapsulation efficiency (89.26%-99.89%) at different ratios (w/v). Increment in nanoencapsulation efficiency and loading capacity according to increase in *Carum copticum* essential oil into chitosan nanoparticle has been presented by Esmaeili & Asgari (2015). However, our investigation displayed better loading capacity as compared to the above mentioned results. More importantly, variation in nanoencapsulation efficiency and loading capacity may depend on the methodology utilized for encapsulation, degree of deacetylation of chitosan, and affinity of EO to be entrapped into the wall matrix (Das, Singh, Dwivedy, Chaudhari, & Dubey, 2021).

3.4. Characterization of nanoemulsion

3.4.1. Structure and size analysis

The representative morphology and diameters of CN-nanoemulsion and CN-PDEO are illustrated in Fig. 1A and B. As can be seen, both CN-nanoemulsion and CN-PDEO exhibited spherical shapes and smooth architectures without cracks, demonstrating good structural integrity. The size of particles in CN-nanoemulsion ranged between 30.47 and

Table 1
Per cent encapsulation efficiency and loading capacity of PDEO loaded into CN-PDEO.

CN: PDEO (w/v)	S-TPP (w/v)	Encapsulation efficiency (%)	Loading capacity (%)
1: 0.0	0.4%	0.00 ± 0.00^{a}	0.00 ± 0.00^{a}
1: 0.2	0.4%	45.81 ± 3.82^{b}	0.68 ± 0.03^{a}
1: 0.4	0.4%	54.24 ± 2.84^{b}	1.68 ± 0.05^{b}
1: 0.6	0.4%	67.62 ± 2.47^{c}	3.95 ± 0.22^{c}
1: 0.8	0.4%	75.05 ± 1.29^{c}	6.04 ± 0.08^{d}
1: 1.0	0.4%	85.84 ± 0.84^{d}	8.26 ± 0.35^{e}

CN = Chitosan; PDEO = *Pimenta dioica* essential oil; S-TPP = Sodium-tripolyphosphate.
Values are expressed as mean (n = 3) ± Standard error (SE);
Different lowercase letters (a–e) in the same column indicate significant differences ($P < 0.05$).

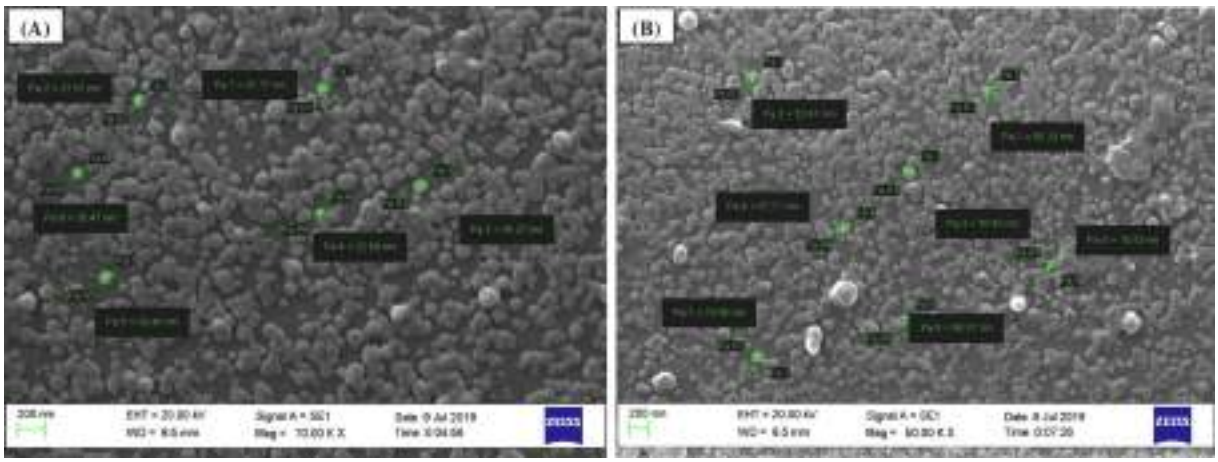

Fig. 1. Scanning electron micrographs (SEM) of (A) chitosan (CN)-nanoemulsion, and (B) CN-nanoemulsion loaded with *Pimenta dioica* essential oil (CN-PDEO).

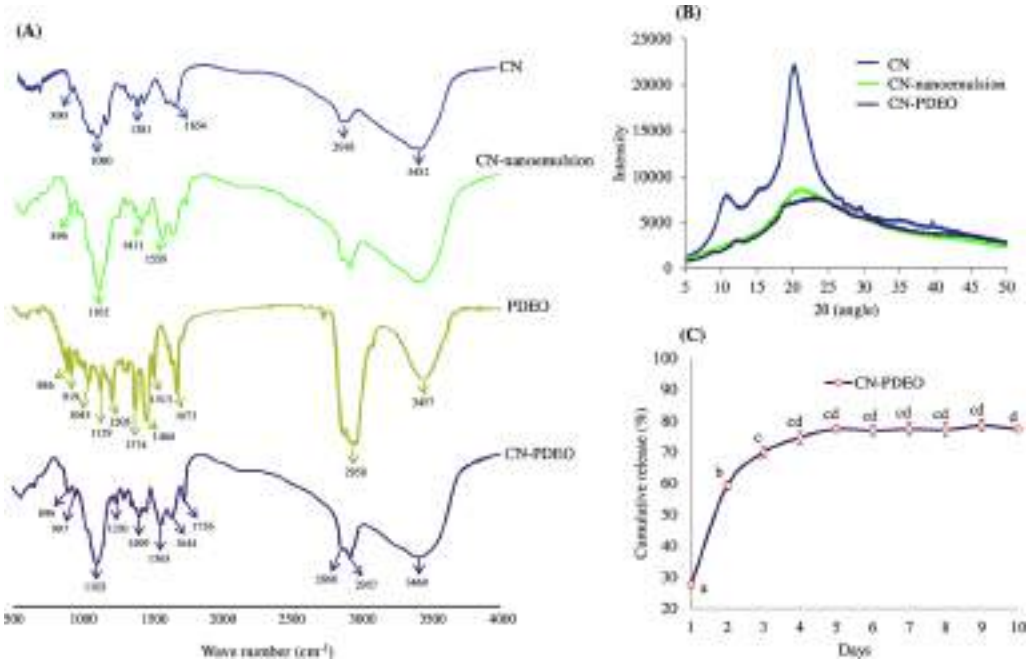

Fig. 2. Characterization of nanoemulsion: (A) Fourier-transform infrared (FTIR) spectra of CN powder, CN-nanoemulsion, *Pimenta dioica* essential oil (PDEO), and CN-nanoemulsion loaded with *Pimenta dioica* essential oil (CN-PDEO), (B) X-ray diffraction (XRD) patterns of chitosan (CN) powder, chitosan (CN)-nanoemulsion and CN-nanoemulsion loaded with *Pimenta dioica* essential oil (CN-PDEO), and (C) *In vitro* release profiles of CN-nanoemulsion loaded with *Pimenta dioica* essential oil (CN-PDEO). The values are presented as mean ± standard error (SE). Bars with different letters indicate significant differences ($P < 0.05$) by Tukey's B test.

51.77 nm. However, the size of the particles was slightly larger (18.53–70.56 nm) when PDEO was loaded into CN-nanoemulsion, which proves successful loading of PDEO into CN. All particle diameters were observed < 100 nm. This observation is in consistence with the morphology previously reported for CN-nanoparticles loaded with oregano EO (Hosseini, Zandi, Rezaei, & Farahmandghavi, 2013), and clove EO (Hasheminejad, Khodaiyan, & Safari, 2019). However, agglomerations were observed in some locations, indicating no phase separation during the sonication process. The aggregation may occur due to interaction between the CN chains or as a result of natural gathering due to inadequate steric stabilization by surfactant present on the surface of CN.

3.4.2. Functional groups and chemical structure analysis

The FTIR spectra of CN, CN-nanoemulsion, PDEO, and CN-PDEO are shown in Fig. 2A. The spectrum of CN showed different peaks at 3452 cm^{-1} due to O—H and N—H stretching, 2918 cm^{-1} due to C—H stretching, 1654 cm^{-1} due to amide I and C═C stretching, 1381 cm^{-1} due to C—N stretching, 1090 cm^{-1} due to C—O—C stretching of glucose ring, and 890 cm^{-1} due to vibration of the pyranose ring. In case of CN-nanoemulsion, a shift in peak intensity from 1090 to 1102 cm^{-1} due to phosphate stretching and two new peaks at 1411 cm^{-1} due to C—N stretching, and 1559 cm^{-1} due to N—H bending were noticed, which was mainly linked to the ionic cross-linkage reaction between the NH_3^+ group of CN and $P_3O_{10}^{-5}$ group of S-TPP. The spectrum of pure PDEO showed numerous peaks including 3457 cm^{-1} due to O—H stretching, 2958 cm^{-1} due to methyl C—H stretching, 1673 cm^{-1} due to alkenyl C═C stretching, 1513 cm^{-1} due to aromatic C═C–C stretching, 1464 cm^{-1} due to methyl C—H bending, 1374 cm^{-1} due to primary and secondary O—H bending, 1205 cm^{-1} due to aromatic C—H bending, 1129 cm^{-1} due to C—C stretching, 1045 cm^{-1} due to primary O—H or C—C stretching, 919 cm^{-1} due to methyl C—H stretching, and 886 cm^{-1} due to C═O-O stretching, which was attributed to the presence of a variety of components in EO, as also verified by GC–MS analysis (Chaudhari et al., 2020a). All the above characteristic peaks appeared in the spectra of CN-PDEO with the slight shift in wave number demonstrating that PDEO was successfully loaded in the CN.

3.4.3. Crystallographic profile analysis

XRD patterns of the CN, CN-nanoemulsion, and CN-PDEO are

presented in Fig. 2B. Pure CN showed two shoulder peaks i.e. one at 10.9°, and second at 20°, corresponding to a relatively high degree of crystallinity, which was endorsed to inter-molecular interactions caused by H-bonds on the –NH and –OH groups in the CN chains (Liu & Liu, 2020). However, no characteristic diffraction peaks were noticed in the CN-nanoemulsion, reflecting destruction of crystallinity (amorphous nature), most probably as a result of ionic interactions between CN and S-TPP (Hosseini, Zandi, Rezaei, & Farahmandghavi, 2013). Widening of peak area with the resultant destruction in CN crystallinity after cross-linking of NH_3 group of CN with S-TPP counter ion during nano-encapsulation has also been reported by Alehosseini, Jafari, & Tabarestani (2021). They also suggested more disarray in CN nanostructure alignment after incorporation of EO leading to formation of imperfect crystal structure. Further, after addition of PDEO, more widening with reduction in peak intensity was noticed, indicating greater disarray of the CN packing structure. This can be attributed to the loading of PDEO into CN.

3.5. *In vitro release properties of PDEO from CN-PDEO*

The release profiles of CN-PDEO at different time intervals (1–10 days) are shown in Fig. 2C. The result showed that release occurred in biphasic way i.e. initial burst release for the first 2 days followed by sustained release for remaining days of assay. The maximum amount of PDEO that could release from the CN-nanoemulsion was approximately 77.33%, indicating that 8.51% of the PDEO out of 85.84% was still entrapped within CN and last for 10 days. The rapid release may be attributed to the leakage of PDEO that was not completely entrapped into CN core or due to the phenomenon of diffusion, where EO moves from high concentration to the low concentration and continues until equilibrium (Anitha et al., 2011). Matshetshe, Parani, Manki, & Oluwafemi (2018) reported similar observation during demonstration of the release behaviour of *Cinnamomum zeylanicum* EO loaded into CN nanoparticles and suggested that burst release at initial stage could be attributed to the release of EO available on the surface of CN, while at second stage (controlled), the release occurred due to the diffusion of the medium into the nano-system, which caused the disintegration of the CN matrix. Hence, the encapsulation of PDEO in CN-nanoemulsion greatly helped to preserve the EO volatility characteristics, which is necessary for the protection of the stored food items over a longer period of storage. This result was further confirmed by determining the antifungal and antiaflatoxigenic effectiveness of the CN-PDEO during *in vitro* and *in vivo* investigations.

3.6. *Efficacy of PDEO and CN-PDEO against moulds and aflatoxin B_1 production*

The results corresponding to the antifungal and antiaflatoxigenic activity of PDEO (authors published work, Chaudhari et al., 2020a) and CN-PDEO against AF-LHP-VS8 at tested concentrations are shown in Fig. 3A. The complete suppression of fungal growth and aflatoxin B_1 production by PDEO was noted at a concentration of 2.5 and 1.5 μL/mL, respectively (Chaudhari et al., 2020a). CN-PDEO displayed better efficacy for inhibition of fungal growth and aflatoxin B_1 secretion at 1.6 and 1.0 μL/mL, respectively (Fig. 3A). In addition, mycelial dry weights also decreased with the increasing concentrations of PDEO and CN-PDEO. Better antifungal activity is related with the size of the nanoemulsion. The size dependent antifungal activity has previously been reported for cinnamon EO nanoemulsion (Pongsumpun, Iwamoto, & Siripatrawan, 2020). The authors reported that the extremely small size of the particles in nanoemulsion was capable of bringing the test EO to the exterior of fungal cells and improved its efficacy. The enhanced antifungal activity of CN-PDEO might also be reflected to the synergistic effect of the PDEO with the CN as well as due to its controlled release from the CN-nanoemulsion (Donsì, Sessa, Mediouni, Mgaidi, & Ferrari, 2011; Hosseini, Zandi, Rezaei, & Farahmandghavi, 2013). Also, the superior

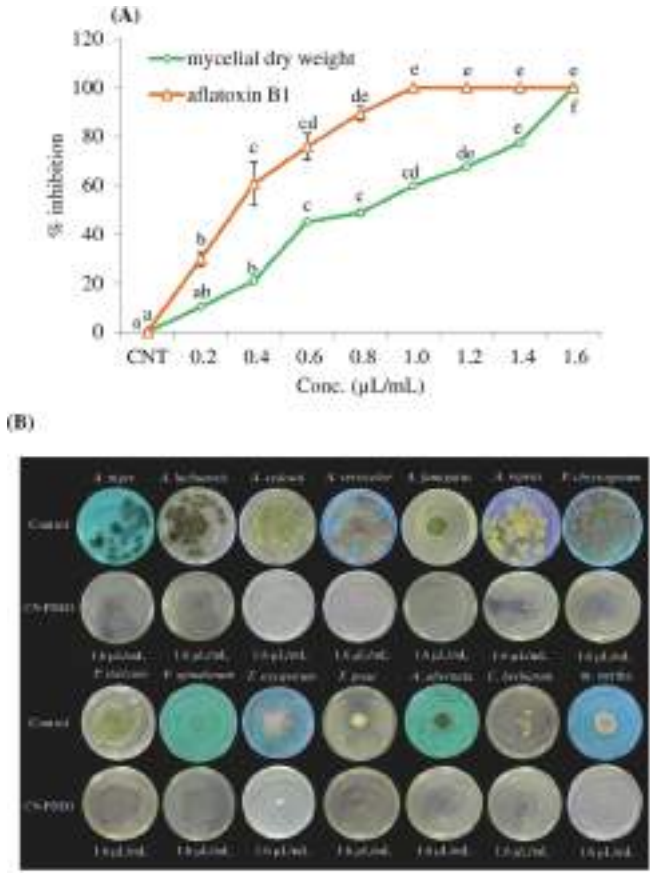

Fig. 3. Effect of different concentrations of CN-nanoemulsion loaded with *Pimenta dioica* essential oil (CN-PDEO) on (A) mycelial growth inhibition of *A. flavus* (AF-LHP-VS8) and aflatoxin B_1 production, (B) antifungal activity of CN-nanoemulsion loaded with *Pimenta dioica* essential oil (CN-PDEO) against other storage moulds at minimum inhibitory concentration (MIC). The values are presented as mean ± standard error (SE). Bars with different letters indicate significant differences ($P < 0.05$) by Tukey's B test.

antifungal activity can be attributed to the improved water solubility of the encapsulated PDEO by enhancing the diffusion rate against test fungus as well as due to the antifungal activity of α-Terpineol, which is the main compound of PDEO used in the present study (Chaudhari et al., 2020b). The complete inhibition of *A. flavus* growth by PDEO and CN-PDEO at 2.5 and 1.6 μL/mL concentrations, respectively can be correlated with the complete suppression of aflatoxin B_1 biosynthesis because partial inhibition (fungistatic) could trigger secondary metabolism as a stress response (Van Long, Joly, & Dantigny, 2016). In addition, PDEO at MIC concentration (2.5 μL/mL) inhibited the growth of 10 other fungi viz., *A. niger*, *A. sydowii*, *A. versicolor*, *A. fumigatus*, *A. repens*, *F. oxysporum*, *F. poae*, *A. alternata*, and mycelia sterilia (Chaudhari et al., 2020a), whereas CN-PDEO at its MIC concentration (1.6 μL/mL) completely inhibited the growth of all 14 tested fungi namely *A. niger*, *A. luchuensis*, *A. sydowii*, *A. versicolor*, *A. fumigatus*, *A. repens*, *P. chrysogenum*, *P. italicum*, *P. spinulosum*, *F. oxysporum*, *F. poae*, *A. alternata*, *C. herbarum*, and mycelia sterilia), exhibiting superior fungitoxic spectrum over its un-encapsulated counterpart (Fig. 3B).

3.7. *Antifungal mode of action of PDEO and CN-PDEO on A. flavus*

In the current study, antifungal mode of action of PDEO and CN-PDEO was evaluated by measuring the ergosterol content, cellular constituent's release, and dysfunction of mitochondrial membrane potential in *A. flavus*. It can be inferred from our previous result that the ergosterol content was decreased significantly with the increasing

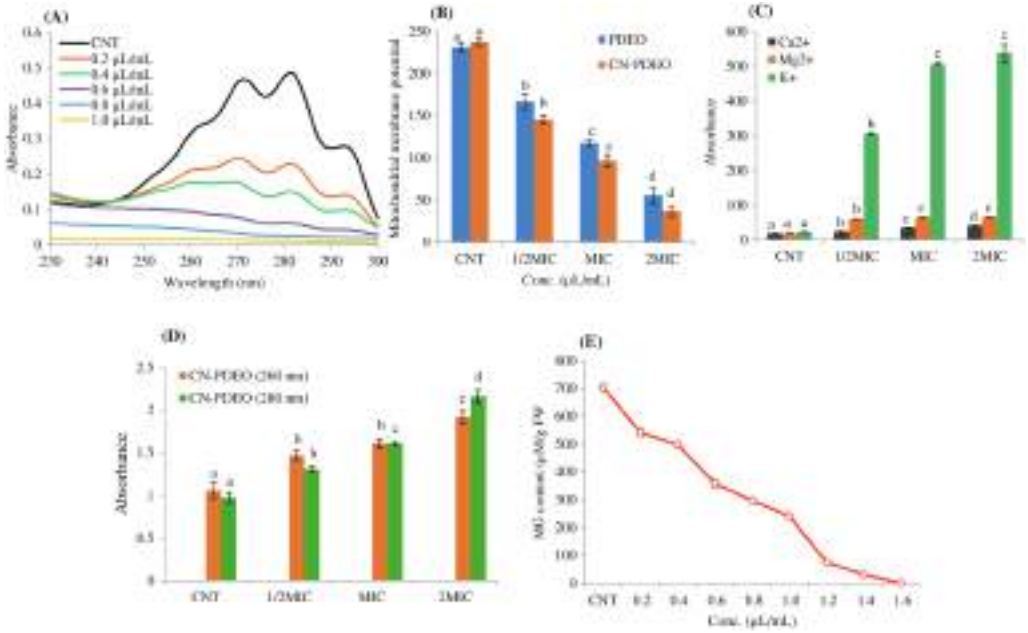

Fig. 4. Effect of different concentrations of CN-nanoemulsion loaded with *Pimenta dioica* essential oil (CN-PDEO) on (A) cellular ergosterol content, and (B) effect of different concentrations of *Pimenta dioica* essential oil (PDEO) and CN-nanoemulsion loaded with *Pimenta dioica* essential oil (CN-PDEO) on mitochondrial membrane potential, (C and D) effect of different concentrations of CN-nanoemulsion loaded with *Pimenta dioica* essential oil (CN-PDEO) on cellular ions leakage and 260 and 280 nm absorbing materials release, and (E) methylglyoxal (MG) content of treated AF-LHP-VS8 cells. The values are presented as mean ± standard error (SE). Bars with different letters indicate significant differences ($P < 0.05$) by Tukey's B test.

concentrations of PDEO (Chaudhari et al., 2020a); however, CN-PDEO exhibited superior efficacy on inhibition of cellular ergosterol biosynthesis at lower concentrations (Fig. 4A). Further, both PDEO and CN-PDEO caused dose-dependent decline in mitochondrial membrane potential (Fig. 4B). This can be attributed to the alteration in proton concentration flowing through the electron transport chain (Grande-Tovar, Chaves-Lopez, Serio, Rossi, & Paparella, 2018). The marked changes in mitochondrial membrane potential have been used as one of the main biochemical hallmarks, especially the energy-coupling condition of mitochondria (Tian et al., 2012). The decrease in mitochondrial membrane potential causes depletion in ATP metabolism by means of the inhibition of enzymes such as mitochondrial ATPase, malate dehydrogenase, and succinate dehydrogenase, which would ultimately inhibit the proton pumping and thus inhibition of acidification with the subsequent cell death (Lunde & Kubo, 2000; Hu, Zhang, Kong, Zao, & Yang, 2017).

Additionally, PDEO enhanced the leakage of important cellular constituents viz., ions such as Ca^{2+}, Mg^{2+} and K^{+}, as well as 260 nm (DNA) and 280 nm (proteins) absorbing materials with the increasing concentrations in contrast to controls (Chaudhari et al., 2020a), while CN-PDEO exposure caused more enhanced leakage (Fig. 4C and D). Moreover, the leakage at 2MIC was higher than that of the MIC, indicating that both PDEO and CN-PDEO at double doses were more destructive than single MIC dose. These results confirmed that PDEO and CN-PDEO may act as antifungal agent via rupturing fungal plasma membrane integrity. It has been reported that lipophilic property of EO coupled with sub-cellular size of CN-PDEO enables PDEO to cross plasma membrane barriers, increases membrane permeability, resulting in the leakage of ions cytoplasmic molecules. Fungal plasma membranes are crucial barriers that defend cells from external injury and maintain homeostasis. Once the integrity of membrane is disturbed, a series of subsequent reactions such as changes in the cytoplasmic pH, dissolution of intracellular substances, and inhibition of normal cellular functioning, leading to programmed cell death (Yilmaz et al., 2019). Earlier studies on CN-nanoemulsion loaded with α-Terpineol, and *Origanum majorana* EO against different aflatoxigenic strains of *A. flavus* have also stated the same antifungal mode of action chiefly by the disruption of fungal plasma membrane (Chaudhari et al., 2020b; Chaudhari et al., 2020c). The exact mechanisms by which CN inhibits fungal growth are still unclear; however, different statements have been proposed. One of the most popular mechanisms is its interaction with the negatively charged components of fungal cells, leading to the leakage of intracellular constituents. Other possible mechanisms suggest that CN may enter the fungal cells, interact with nucleic acids (especially DNA), alter its conformation, and chelate with micro- and macronutrients, leading to the inhibited transcription and translation (Sajomsang, Gonil, Saesoo, & Ovatlarnporn, 2012). The antifungal mechanism of action of CN has also been suggested to be related with the alteration in cell wall morphogenesis, interfering directly with the enzymes responsible for fungal growth and development.

3.8. Antiaflatoxigenic mode of action of PDEO and CN-PDEO on A. flavus

To get more insight on the aflatoxin B_1 inhibitory activity of CN-PDEO, the intracellular concentration of aflatoxin stimulatory substrate i.e. MG in AF-LHP-VS8 was analyzed. In our present study, we observed that PDEO caused concentration dependent inhibition of cellular MG, which was not completely inhibited even at MIC dose (Chaudhari et al., 2020a). However, in the present investigation, CN-PDEO presented enhanced efficacy at lower doses and caused complete inhibition of intracellular MG at MIC concentration (Fig. 4E). It has been reported that MG in *A. flavus* caused an enhancement in aflatoxin B_1 biosynthesis, possibly via modulating the expression of master *aflR* gene (Chen, Brown, Damann, & Cleveland, 2004). Further, inhibition of MG may lead to the inhibition of aflatoxin production in *A. flavus* as reported previously (Upadhyay et al., 2018; Singh, Das, Dwivedy, Rathore, & Dubey, 2019). Hence, it is possible that the antiaflatoxigenic activity of CN-PDEO might be linked with the inhibition of MG biosynthesis and the downregulation of gene *aflR* involved in aflatoxin biosynthesis. This result may extend our understanding of novel antiaflatoxigenic target that could be exploited by agricultural scientists for the production of aflatoxin resistant crop varieties through green-transgenic approach.

3.9. In vivo aflatoxin B_1 inhibitory efficacy of PDEO and CN-PDEO in food system

Currently, several published articles are available reporting the efficacy of EOs and their nanoemulsions against mycotoxin production; however, majority of the results so far have come from *in vitro* conditions, which do not allow us predicting the results under real conditions

as generally found during conventional storage; while such research is vital for understanding of their actual preservative efficacy. Therefore, efforts have been made to evaluate the preservative efficacy of PDEO and CN-PDEO in maize to find out its actual effectiveness in protection of stored food samples from aflatoxin B_1 contamination. The antiaflatoxigenic activity of PDEO and CN-PDEO was observed after one year of treatment in closed container system at their respective MIC and 2MIC concentrations. The results obtained from HPLC analysis (chromatogram not shown) clearly evidenced that PDEO and CN-PDEO at taken concentration showed a remarkable efficacy against aflatoxin B_1 contamination. The aflatoxin B_1 content in control set was found to be 112.94 μg/Kg. The extremely high aflatoxin B_1 concentration detected in control sample indicated that management strategies should be urgently needed for use at the postharvest stage. However, PDEO at MIC concentration caused 68.64% protection (aflatoxin B_1 amount 35.42 μg/kg) of fumigated maize from aflatoxin B_1 contamination, while fumigation at 2MIC caused up to 77.81% protection (aflatoxin B_1 amount 24.56 μg/kg). Interestingly, CN-PDEO caused up to 98.89% (aflatoxin B_1 amount 1.25 μg/kg) and 100% protection (no aflatoxin B_1) of treated maize samples from aflatoxin B_1 contamination at MIC and 2MIC concentration, respectively. Interestingly, the antiaflatoxigenic activity of the CN-PDEO persisted up to one year, thus enabling its application for food safety.

3.10. Determination of lipid peroxidation in stored maize

The determination of TBA-reactive substances (TBARS) by measuring MDA content is one of the most widely used methods to evaluate the extent of lipid peroxidation in stored foods. The high levels of MDA indicate higher degree of lipid peroxidation. Both PDEO and CN-PDEO caused dose dependent inhibition of MDA level in the treated sets after one year of storage. The lowest level of TBARS was obtained at 2MIC concentrations of PDEO and CN-PDEO with MDA content 129.6 μg MDA/g FW and 68.10 μg MDA/g FW, respectively, while the highest value was obtained for the control sample with MDA content 409 μg MDA/g FW (Fig. 5A). Interestingly, CN-PDEO was more effective in inhibiting the process of lipid peroxidation than PDEO. The effect of EO encapsulated in CN polymer on lipid peroxidation inhibition of stored food product has also been described by others (Upadhyay, Singh, Dwivedy, Chaudhari, & Dubey, 2021).

3.11 . Phytotoxicity assessment of PDEO and CN-PDEO in maize

The phytotoxicity test revealed that both PDEO and CN-PDEO had no negative impact on germination ability of maize seeds, showing 100% germinating even after one year of storage treatment (Chaudhari et al., 2020a; Fig. 5B). Hence, PDEO and CN-PDEO treated maize samples may be used for sowing as well as consumption purposes by the farmers and consumers.

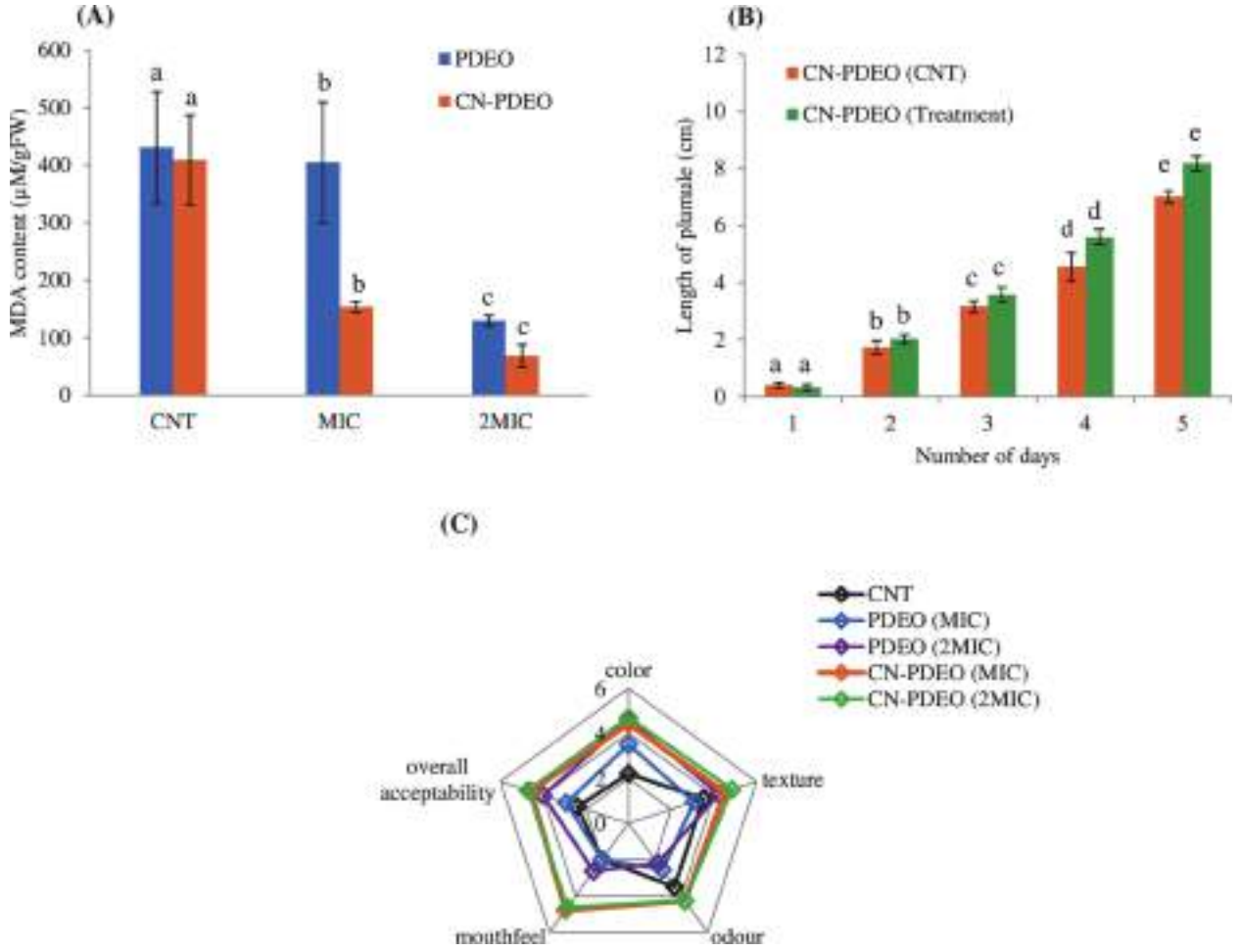

Fig. 5. (A) Effect of *Pimenta dioica* essential oil (PDEO) and CN-nanoemulsion loaded with *Pimenta dioica* essential oil (CN-PDEO) on lipid peroxidation, (B) phytotoxicity assessment of CN-nanoemulsion loaded with *Pimenta dioica* essential oil (CN-PDEO) on maize seeds, and (C) sensory attributes of maize samples treated with minimum inhibitory concentration (MIC) and double minimum inhibitory concentration (2MIC) of *Pimenta dioica* essential oil (PDEO) and CN-nanoemulsion loaded with *Pimenta dioica* essential oil (CN-PDEO). The values are presented as mean ± standard error (SE). Bars with different letters indicate significant differences ($P < 0.05$) by Tukey's B test.

3.12. Safety profile assessment: Oral acute toxicity study of PDEO and CN-PDEO

In order to ensure the safety of PDEO and CN-PDEO for further application as antifungal agent in food system, its toxicity was evaluated on mice model. Because of the lack of studies related to the safety profile, it does not seem that the PDEO and CN-PDEO can be used for food preservation. In both the controls (positive and negative), all mice were found alive and active without any symptoms of toxicity. However, in treatment groups, the mortality increased with the increasing doses of PDEO and CN-PDEO from 100 − 1000 μL/30 g body weight. The obtained median lethal dose (LD_{50}) of PDEO and CN-PDEO was converted into μL/Kg body weight of mice. The estimated LD_{50} value of PDEO and CN-PDEO as calculated from the logarithmic regression analysis of the dose–response curve was found to be 9,316 μL/Kg and 10,072 μL/Kg body weight, respectively. The results of this study confirmed that both PDEO and CN-PDEO were non-toxic substance, and could be used for safe preservation of stored food items.

3.13. Sensory analysis of PDEO and CN-PDEO treated maize

A sensory analysis was run to further check the acceptability of the maize samples treated with PDEO and CN-PDEO at established concentrations. The average scores marked by the assessors for all the evaluated attributes are shown in Fig. 5C. The results showed that maize samples treated with MIC concentration of PDEO obtained lower scores for color, texture, odour, mouth feel, and overall acceptability; however, at 2MIC concentration, there were little improvement in the scores for color, texture, and overall acceptability (Fig. 5C). The lower scores for un-encapsulated PDEO may be attributed to its aromatic profile that can be absorbed by the treated food sample, eventually causing decline in sensory scores. However, CN-PDEO exhibited satisfactory scores for all the parameters viz., color, texture, odour, mouth feel, and the overall acceptability at both MIC and 2MIC doses. This result supported the facts that nanoencapsulation could offer distinct advantages to overcome the limitations related with organoleptic perceptions, as they can optimize and allow in maintaining the effective concentration of a test EO in treated food system via controlled release mechanism, thereby providing complete protection without altering the sensory properties of final products (Hossain et al., 2019).

4. Conclusion

The present research offers a frontier method for application of *Pimenta dioica* essential oil (PDEO) loaded chitosan (CN) nanoemulsion (CN-PDEO) synthesized by homogenization assisted ionic-gelation against fungal infestation, aflatoxin B_1 contamination, and lipid peroxidation not only for maize, but also for other food commodities during postharvest storage. The first time developed nanoformulation (CN-PDEO) could suitably serve as nano-based green alternative of synthetic preservatives (posing adverse effects on human health and environment) without altering the natural attributes of food commodities. More importantly, the biochemical mode of action would reveal the site of antifungal and antiaflatoxigenic action and could be helpful in determining the minimal dose of CN-PDEO. The controlled release of PDEO from CN-PDEO could facilitate the long term protection of stored food commodities. Most notably, the cost-benefit ratio and the toxicity if any, arising from the nano-sized CN-PDEO, should be taken into consideration for both the nanoemulsion and lyophilized powders of CN-PDEO to be supplemented with food commodities in order to protect them from fungal and mycotoxin contamination prior to large scale application.

Ethical statement

The experiment on selected animal model was conducted strictly according to the institutional ethical standards and prior approval was taken from the ethical committee of the Banaras Hindu University, India.

CRediT authorship contribution statement

Anand Kumar Chaudhari: Conceptualization, Writing – original draft, Investigation, Funding acquisition. **Vipin Kumar Singh:** Writing - review & editing, Writing - original draft. **Somenath Das:** Methodology, Validation, Data curation. **Deepika:** Methodology, Formal analysis. **Nawal Kishore Dubey:** Writing - review & editing, Supervision.

Declaration of Competing Interest

The authors declare that they have no known competing financial interests or personal relationships that could have appeared to influence the work reported in this paper.

Acknowledgements

This research was financially supported by the Council of Scientific and Industrial Research (CSIR) [Grant no. 09/013(0678)/2017–EMR–I], New Delhi, India. The authors also thank Head, Department of Botany, ISLS for providing laboratory facilities and CIF, Indian Institute of Technology, Banaras Hindu University, Varanasi for SEM, FTIR and XRD analysis.

References

Adams, R. P. (2007). *Identification of essential oil components by gas chromatography/mass spectrometry* (vol. 18,, 803–806.

Alehosseini, E., Jafari, S. M., & Tabarestani, H. S. (2021). Production of d-limonene-loaded Pickering emulsions stabilized by chitosan nanoparticles. *Food Chemistry, 354*, Article 129591.

Ali, H., Al-Khalifa, A. R., Aouf, A., Boukhebti, H., & Farouk, A. (2020). Effect of nanoencapsulation on volatile constituents, and antioxidant and anticancer activities of Algerian *Origanum glandulosum* Desf. essential oil. *Scientific Reports, 10*, 1–9.

Anitha, A., Deepagan, V. G., Divya Rani, V. V., Menon, D., Nair, S. V., & Jayakumar, R. (2011). Preparation, characterization, in vitro drug release and biological studies of curcumin loaded dextran sulphate–chitosan nanoparticles. *Carbohydrate Polymers, 84*(3), 1158–1164.

Barata, L. E. S., dos Santos, B. C. B., Marques, F. A., Baroni, A. C. M., de Oliveira, P. R., Einloft, P., … Guerrero, P. G. (2011). Seasonal variation of the volatile constituents from leaves of *Pimenta pseudocaryophyllus* (Gomes). *Journal of Essential Oil Research, 23*(4), 54–57.

Benjemaa, M., Neves, M. A., Falleh, H., Isoda, H., Ksouri, R., & Nakajima, M. (2018). Nanoencapsulation of *Thymus capitatus* essential oil: Formulation process, physical stability characterization and antibacterial efficiency monitoring. *Industrial Crops and Products, 113*, 414–421.

Chaudhari, A. K., Dwivedy, A. K., Singh, V. K., Das, S., Singh, A., & Dubey, N. K. (2019). Essential oils and their bioactive compounds as green preservatives against fungal and mycotoxin contamination of food commodities with special reference to their nanoencapsulation. *Environmental Science and Pollution Research, 26*(25), 25414–25431.

Chaudhari, A. K., Singh, A., Kumar Singh, V., Kumar Dwivedy, A., Das, S., Grace Ramsdam, M., … Kishore Dubey, N. (2020b). Assessment of chitosan biopolymer encapsulated α-Terpineol against fungal, aflatoxin B_1 (AFB_1) and free radicals mediated deterioration of stored maize and possible mode of action. *Food Chemistry, 311*, 126010.

Chaudhari, A. K., Singh, V. K., Das, S., & Dubey, N. K. (2021). Nanoencapsulation of essential oils and their bioactive constituents: A novel strategy to control mycotoxin contamination in food system. *Food and Chemical Toxicology, 149*, 112019. https://doi.org/10.1016/j.fct.2021.112019

Chaudhari, A. K., Singh, V. K., Das, S., Deepika, Prasad, J., Dwivedy, A. K., & Dubey, N. K. (2020c). Improvement of *in vitro* and *in situ* antifungal, AFB_1 inhibitory and antioxidant activity of *Origanum majorana* L. essential oil through nanoemulsion and recommending as novel food preservative. *Food and Chemical Toxicology, 143*, 111536. https://doi.org/10.1016/j.fct.2020.111536

Chaudhari, A. K., Singh, V. K., Dwivedy, A. K., Das, S., Upadhyay, N., Singh, A., … Dubey, N. K. (2020a). Chemically characterised *Pimenta dioica* (L.) Merr. essential oil as a novel plant based antimicrobial against fungal and aflatoxin B1 contamination of stored maize and its possible mode of action. *Natural Product Research, 34*(5), 745–749.

Chen, Z.-Y., Brown, R. L., Damann, K. E., & Cleveland, T. E. (2004). Identification of a maize kernel stress-related protein and its effect on aflatoxin accumulation. *Phytopathology, 94*(9), 938–945.

da Silva Bomfim, N., Nakassugi, L. P., Oliveira, J. F. P., Kohiyama, C. Y., Mossini, S. A. G., Grespan, R., & Machinski, M., Jr (2015). Antifungal activity and inhibition of

fumonisin production by *Rosmarinus officinalis* L. essential oil in *Fusarium verticillioides* (Sacc.) Nirenberg. *Food Chemistry, 166*, 330–336.

Das, S., Kumar Singh, V., Kumar Dwivedy, A., Kumar Chaudhari, A., Deepika, & Kishore Dubey, N. (2021b). Nanostructured *Pimpinella anisum* essential oil as novel green food preservative against fungal infestation, aflatoxin B_1 contamination and deterioration of nutritional qualities. *Food Chemistry, 344*, 128574. https://doi.org/10.1016/j.foodchem.2020.128574

Das, S., Singh, V. K., Dwivedy, A. K., Chaudhari, A. K., Deepika, & Dubey, N. K. (2021a). Eugenol loaded chitosan nanoemulsion for food protection and inhibition of Aflatoxin B1 synthesizing genes based on molecular docking. *Carbohydrate Polymers, 255*, 117339.

Das, S., Singh, V. K., Dwivedy, A. K., Chaudhari, A. K., Upadhyay, N., Singh, P., … Dubey, N. K. (2019). Encapsulation in chitosan-based nanomatrix as an efficient green technology to boost the antimicrobial, antioxidant and in situ efficacy of *Coriandrum sativum* essential oil. *International Journal of Biological Macromolecules, 133*, 294–305.

Deepika, Chaudhari, A. K., Singh, A., Das, S., & Dubey, N. K. (2021). Nanoencapsulated *Petroselinum crispum* essential oil: Characterization and practical efficacy against fungal and aflatoxin contamination of stored chia seeds. *Food Bioscience, 42*, 101117. https://doi.org/10.1016/j.fbio.2021.101117

Dima, C., Cotărlet, M., Alexe, P., & Dima, S. (2014). Microencapsulation of essential oil of pimento [*Pimenta dioica* (L) Merr.] by chitosan/k-carrageenan complex coacervation method. *Innovative Food Science and Emerging Technologies, 22*, 203–211.

Donsì, F., Sessa, M., Mediouni, H., Mgaidi, A., & Ferrari, G. (2011). Encapsulation of bioactive compounds in nanoemulsion-based delivery systems. *Procedia Food Science, 1*, 1666–1671.

Esmaeili, A., & Asgari, A. (2015). *In vitro* release and biological activities of Carum copticum essential oil (CEO) loaded chitosan nanoparticles. *International Journal of Biological Macromolecules, 81*, 283–290.

Ghaderi-Ghahfarokhi, M., Barzegar, M., Sahari, M. A., Ahmadi Gavlighi, H., & Gardini, F. (2017). Chitosan-cinnamon essential oil nano-formulation: Application as a novel additive for controlled release and shelf life extension of beef patties. *International Journal of Biological Macromolecules, 102*, 19–28.

Grande-Tovar, C. D., Chaves-Lopez, C., Serio, A., Rossi, C., & Paparella, A. (2018). Chitosan coatings enriched with essential oils: Effects on fungi involved in fruit decay and mechanisms of action. *Trends in Food Science and Technology, 78*, 61–71.

Hasheminejad, N., Khodaiyan, F., & Safari, M. (2019). Improving the antifungal activity of clove essential oil encapsulated by chitosan nanoparticles. *Food Chemistry, 275*, 113–122.

Hossain, F., Follett, P., Salmieri, S., Vu, K. D., Fraschini, C., & Lacroix, M. (2019). Antifungal activities of combined treatments of irradiation and essential oils (EOs) encapsulated chitosan nanocomposite films in *in vitro* and *in situ* conditions. *International Journal of Food Microbiology, 295*, 33–40.

Hosseini, S. F., Zandi, M., Rezaei, M., & Farahmandghavi, F. (2013). Two-step method for encapsulation of oregano essential oil in chitosan nanoparticles: Preparation, characterization and *in vitro* release study. *Carbohydrate Polymers, 95*(1), 50–56.

Hu, Y., Zhang, J., Kong, W., Zhao, G., & Yang, M. (2017). Mechanisms of antifungal and anti-aflatoxigenic properties of essential oil derived from turmeric (*Curcuma longa* L.) on *Aspergillus flavus*. *Food Chemistry, 220*, 1–8.

Hussein, A. M. S., Kamil, M. M., Lotfy, S. N., Mahmoud, K. F., Mehaya, F. M., & Mohammad, A. A. (2017). Influence of nano-encapsulation on chemical composition, antioxidant activity and thermal stability of rosemary essential oil. *American Journal of Food Technology, 12*(3), 170–177.

Jemaa, M. B., Falleh, H., Neves, M. A., Isoda, H., Nakajima, M., & Ksouri, R. (2017). Quality preservation of deliberately contaminated milk using thyme free and nanoemulsified essential oils. *Food Chemistry, 217*, 726–734.

Kordali, S., Cakir, A., Ozer, H., Cakmakci, R., Kesdek, M., & Mete, E. (2008). Antifungal, phytotoxic and insecticidal properties of essential oil isolated from Turkish Origanum acutidens and its three components, carvacrol, thymol and p-cymene. *Bioresource Technology, 99*(18), 8788–8795.

Liu, T., & Liu, L. (2020). Fabrication and characterization of chitosan nanoemulsions loading thymol or thyme essential oil for the preservation of refrigerated pork. *International Journal of Biological Macromolecules, 162*, 1509–1515.

Lunde, C. S., & Kubo, I. (2000). Effect of polygodial on the mitochondrial ATPase of *Saccharomyces cerevisiae*. *Antimicrobial Agents Chemotherapy, 44*(7), 1943–1953.

Matshetshe, K. I., Parani, S., Manki, S. M., & Oluwafemi, O. S. (2018). Preparation, characterization and *in vitro* release study of β-cyclodextrin/chitosan nanoparticles loaded *Cinnamomum zeylanicum* essential oil. *International Journal of Biological Macromolecules, 118*, 676–682.

Ostry, V., Malir, F., Toman, J., & Grosse, Y. (2017). Mycotoxins as human carcinogens—the IARC Monographs classification. *Mycotoxin Research, 33*(1), 65–73.

Pitarević, I., Kuftinec, J., Blažević, N., & Kuštrak, D. (1984). Seasonal variation of essential oil yield and composition of dalmatian sage, Salvia officinalis. *Journal of Natural Products, 47*(3), 409–412.

Pongsumpun, P., Iwamoto, S., & Siripatrawan, U. (2020). Response surface methodology for optimization of cinnamon essential oil nanoemulsion with improved stability and antifungal activity. *Ultrasonics Sonochemistry, 60*, 104604.

Sajomsang, W., Gonil, P., Saesoo, S., & Ovatlarnporn, C. (2012). Antifungal property of quaternized chitosan and its derivatives. *International Journal of Biological Macromolecules, 50*(1), 263–269.

Sheijooni-Fumani, N., Hassan, J., & Yousefi, S. R. (2011). Determination of aflatoxin B1 in cereals by homogeneous liquid–liquid extraction coupled to high performance liquid chromatography-fluorescence detection. *Journal of Separation Science, 34*(11), 1333–1337.

Singh, V. K., Das, S., Dwivedy, A. K., Rathore, R., & Dubey, N. K. (2019). Assessment of chemically characterized nanoencapuslated *Ocimum sanctum* essential oil against aflatoxigenic fungi contaminating herbal raw materials and its novel mode of action as methyglyoxal inhibitor. *Postharvest Biology and Technology, 153*, 87–95.

Tian, J., Ban, X., Zeng, H., He, J., Chen, Y., & Wang, Y. (2012). The mechanism of antifungal action of essential oil from dill (*Anethum graveolens* L.) on *Aspergillus flavus*. *PloS one, 7*, Article e30147.

Upadhyay, N., Singh, V. K., Dwivedy, A. K., Chaudhari, A. K., & Dubey, N. K. (2021). Assessment of nanoencapsulated *Cananga odorata* essential oil in chitosan nanopolymer as a green approach to boost the antifungal, antioxidant and *in situ* efficacy. *International Journal of Biological Macromolecules, 171*, 480–490.

Upadhyay, N., Singh, V. K., Dwivedy, A. K., Das, S., Chaudhari, A. K., & Dubey, N. K. (2018). *Cistus ladanifer* L. essential oil as a plant based preservative against molds infesting oil seeds, aflatoxin B_1 secretion, oxidative deterioration and methylglyoxal biosynthesis. *LWT-Food Science & Technology, 92*, 395–403.

Nguyen Van Long, N., Joly, C., & Dantigny, P. (2016). Active packaging with antifungal activities. *International Journal of Food Microbiology, 220*, 73–90.

Yilmaz, M. T., Yilmaz, A., Akman, P. K., Bozkurt, F., Dertli, E., Basahel, A., … Sagdic, O. (2019). Electrospraying method for fabrication of essential oil loaded-chitosan nanoparticle delivery systems characterized by molecular, thermal, morphological and antifungal properties. *Innovative Food Science and Emerging Technologies, 52*, 166–178.